Organometallic Cluster Complexes with Face-Capping Arene Ligands. 8. Nucleophilic Reactivity of Cluster Complexes with Face-Capping Arene Ligands: Metal vs Ligand Protonation†

Hubert Wadepohl,*[1a] Maria José Calhorda,*[1b,c] Michael Herrmann,[1a] Christof Jost,[1a] Pedro E. M. Lopes,[1b] and Hans Pritzkow[1a]

Anorganisch-Chemisches Institut der Ruprecht-Karls-Universität, Im Neuenheimer Feld 270, D-69120 Heidelberg, Germany, Instituto de Tecnologia Química e Biológica (ITQB), Rua de Quinta Grande, 6, Apartado 127, 2780 Oeiras, Portugal, and Instituto Superior Técnico (IST), Lisboa, Portugal

Received July 10, 1996[⊗]

Protonation of some cluster complexes with face-capping arene ligands has been studied. The complexes $[(CpCo)_3(\mu_3\text{-}\eta^2{:}\eta^2{:}\eta^2\text{-arene})]$ [arene = isopropylbenzene (**1a**), 1,4-diethylbenzene (**1b**), 1,2-diphenylethane (**1c**), 1,1-diphenylethane (**1d**)] are protonated at the metal clusters to afford the hydrido cluster cations $[(\mu_3\text{-H})(CpCo)_3(\mu_3\text{-}\eta^2{:}\eta^2{:}\eta^2\text{-arene})]^+$ (**3a**−**d**). The crystal structure of **3d**$[CF_3COO]^-\cdot H_2O$ has been determined. In marked contrast, derivatives with μ_3-arenes bearing unsaturated substituents [arene = α-methylstyrene (**2a**), *β*-methylstyrene (**2b**), *p*-methoxystyrene (**2c**)] take up a proton at the *β*-carbon atom of the side chain to give the novel metal cluster stabilized benzyl cations $[(CpCo)_3\{\mu_3\text{-}\alpha,1\text{-}\eta^2{:}2\text{-}4\text{-}\eta^3{:}4\text{-}6\text{-}\eta^3\text{-}(4\text{-}R^3)\text{-}C_6H_4(1\text{-}C(CH_2R^1)(R^2))\}]^+$ (**4a**−**c**). On attempted crystallization as a tetrafluoroborate, the derivative **4a** with a protonated α-methylstyrene ligand is converted to the paramagnetic $[(CpCo)_3\{\mu_3\text{-}\eta^2{:}\eta^2{:}\eta^2\text{-}(\alpha\text{-methylstyrene})\}]^+$ (**2a**$^+$), the crystal structure of which is reported. The different sites of protonation for **1** and **2** are explained by an extended Hückel (EH) MO study, using both charge and overlap control arguments. The paramagnetic cation was studied, and its geometry found to agree very well with the experimentally determined structure described for **2a**$^+$, suggesting that it is indeed this the species being observed. A detailed analysis of the geometrical preferences of the protonation products **4** was carried out, using EH and density functional methods. A slipped eclipsed arrangement of a nonplanar η^7-benzyl ligand on top of the Co_3 cluster with the side chain bent away appears to be energetically favored over a staggered substituted benzene.

Introduction

Complexation of arenes to metal carbonyl fragments, notably $(CO)_3Cr$, activates them to nucleophilic attack.[2] Benzene also shows enhanced nucleophilicity when coordinated to a metal carbonyl cluster in the apical (η^6) or trimetal face-capping (facial, $\mu_3\text{-}\eta^2{:}\eta^2{:}\eta^2$) bonding mode.[3,4] For example, phenyllithium adds to $[Ru_6C(CO)_{12}(\eta^6\text{-}C_6H_6)(\mu_2\text{-}\eta^2{:}\eta^2\text{-}C_6H_8)]$ and $[Ru_6C(CO)_{11}(\eta^6\text{-}C_6H_6)(\mu_3\text{-}\eta^2{:}\eta^2{:}\eta^2\text{-}C_6H_6)]$ to give the anionic cluster complexes $[Ru_6C(CO)_{12}(\eta^5\text{-}C_6H_6Ph)(\mu_2\text{-}\eta^2{:}\eta^2\text{-}C_6H_8)]^-$ and $[Ru_6C(CO)_{11}(\eta^5\text{-}C_6H_6Ph)(\mu_3\text{-}\eta^2{:}\eta^2{:}\eta^2\text{-}C_6H_6)]^-$, respectively, with *exo* phenyl substituted η^5-cyclohexadienyl ligands.[5] Quite interestingly, in the case of $[Ru_6C(CO)_{14}(\eta^6\text{-}C_6H_6)]$ even two phenyl[5] or methyl[5b] anions are added to the 1,4-positions, and the dianions $[Ru_6C(CO)_{14}(\eta^4\text{-}C_6H_6R_2)]^{2-}$ are formed. The μ-benzene ligand in the triosmium cluster complex $[\{(CO)_3Os\}_3(\mu_3\text{-}\eta^2{:}\eta^2{:}\eta^2\text{-}C_6H_6)]$ is also converted into a face-capping *exo*-substituted cyclohexadienyl ligand upon treatment with carbanions (MeLi, PhLi) or $LiBXEt_3$ (X = H, D).[6]

In contrast to the (μ_3-benzene)triosmium carbonyl cluster complex, the complexes $[(CpCo)_3(\mu_3\text{-}\eta^2{:}\eta^2{:}\eta^2\text{-arene})]$ (**1**, **2**)[7] (Chart 1) do not exhibit a pronounced nucleophilic behavior of the face-capping arene nucleus. Simple derivatives with μ_3-alkyl- and alkenylbenzene ligands do not react with RLi (R = Me, Ph).[3,7b] Further activation with a fluorine substituent has to be provided in order to achieve nucleophilic substitution reactions.[8]

† Part 7: Reference 8.
⊗ Abstract published in *Advance ACS Abstracts,* November 15, 1996.

(1) (a) Universität Heidelberg. (b) ITQB. (c) IST.

(2) (a) Pauson, P. L. in *Methoden der organischen Chemie (Houben-Weyl)*; Falbe, J., Ed., Thieme: Stuttgart, Germany, 1986; Vol. E18, Chapter II. (b) Watts, W. E. In *Comprehensive Organometallic Chemistry*; Wilkinson, G., Stone, F. G. A., Abel, E. W., Eds.; Pergamon: Oxford, U.K., 1982; Vol. 8, Chapter 59. (c) Davies, S. G. *Organotransition Metal Chemistry: Application to Organic Synthesis*; Pergamon: Oxford, U.K., 1982; Chapter 4.1.6, 4.2.4. (d) Kane-Maguire, L. A. P.; Honig, E. D.; Sweigart, D. A. *Chem. Rev.* **1984**, *84*, 525.

(3) Wadepohl, H. *Angew. Chem.* **1992**, *104*, 253; *Angew. Chem., Int. Ed. Engl.* **1992**, *31*, 247 and references cited therein.

(4) Braga, D.; Dyson, P. J.; Grepioni, F.; Johnson, B. F. G. *Chem. Rev.* **1994**, *94*, 1585 and references cited therein.

(5) (a) Borchert, T.; Lewis, J.; Pritzkow, H.; Raithby, P. R.; Wadepohl, H. *J. Chem. Soc., Dalton Trans.* **1995**, 1061. (b) Borchert, T.; Lewis, J.; Pritzkow, H.; Raithby, P. R.; Shields, G. P.; Wadepohl, H. Manuscript in preparation.

(6) (a) Gallop, M. A.; Johnson, B. F. G.; Lewis, J.; Wright, A. H. *J. Chem. Soc., Dalton Trans.* **1989**, 481; (b) Edwards, A. J.; Gallop, M. A.; Johnson, B. F. G.; Köhler, J. U.; Lewis, J.; Raithby, J. R. *Angew. Chem.* **1994**, *106*, 1166; *Angew. Chem., Int. Ed. Engl.* **1994**, *33*, 1093.

(7) (a) Wadepohl, H.; Büchner, K.; Pritzkow, H. *Angew. Chem.* **1987**, *99*, 1294; *Angew. Chem., Int. Ed. Engl.* **1987**, *26*, 1259. (b) Wadepohl, H.; Büchner, K.; Herrmann, M.; Pritzkow, H. *Organometallics* **1991**, *10*, 861. (c) Wadepohl, H.; Borchert, T.; Büchner, K.; Herrmann, M.; Paffen, F.-J.; Pritzkow, H. *Organometallics* **1995**, *14*, 3817.

(8) Wadepohl, H.; Borchert, T.; Pritzkow, H. *J. Organomet. Chem.* **1996**, *516*, 187.

S0276-7333(96)00569-9 CCC: $12.00

Chart 1

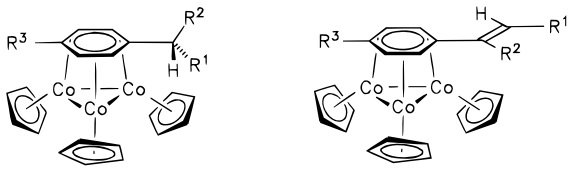

1a, $R^1 = R^2 = Me, R^3 = H$
1b, $R^1 = H, R^2 = Me, R^3 = Et$
1c, $R^1 = R^3 = H, R^2 = CH_2Ph$
1d, $R^1 = Me, R^2 = Ph, R^3 = H$

2a, $R^1 = R^3 = H, R^2 = Me$
2b, $R^1 = Me, R^2 = R^3 = H$
2c, $R^1 = R^2 = H, R^3 = OMe$
2d, $R^1 = R^3 = H, R^2 = Ph$
2e, $R^1 = H, R^2 = Me, R^3 = F$

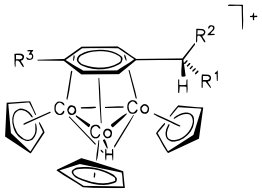

3a, $R^1 = R^2 = Me, R^3 = H$
3b, $R^1 = H, R^2 = Me, R^3 = Et$
3c, $R^1 = R^3 = H, R^2 = CH_2Ph$
3d, $R^1 = Me, R^2 = Ph, R^3 = H$

Here we wish to report the results of a study of the very different reactivities of **1** and **2** with the most simple electrophile, the proton.

Results

(A) Protonation of the Cluster Complexes [(CpCo)$_3$(μ_3-R^{3}C$_6$H$_4${C(H)(R^1)(R^2)}] (1a−d). (a) Syntheses and Spectra. After treatment of CD_2Cl_2 solutions of **1a**−**d** with excess of CF_3COOH, the changes in the ^{1}H NMR spectra indicated immediate and complete formation of the hydrido cluster cations **3a**−**d**. Excess acid could be removed by evaporation of all volatiles *in vacuo* and redissolution of the oily residues. **3c**,**d** were also prepared in a preparative scale using CF_3COOH or aqueous HPF_6 as proton donors. Yields were quantitative; however only oils were obtained, which did not crystallize from methylene chloride or thf. The tetraphenylborates of **3c**,**d** were formed after metathesis of the trifluoroacetates or hexafluorophosphates with $NaBPh_4$ and could be isolated as black crystalline solids in about 40% yield. Deprotonation of **3** to give the neutral starting materials **1** was effected by sodium hydroxide in thf.

The structures of the complexes **3a**−**d** were established by spectroscopic means and, in the case of **3d**, by a single-crystal X-ray structure determination of a trifluoroacetate hydrate. ^{1}H and ^{13}C NMR spectroscopic data are given in Tables 1 and 2. For comparison, the corresponding data for the starting materials **1a**−**d** are also included in the tables. At room temperature and above, the number and multiplet structure of the ^{1}H and ^{13}C resonances due to the μ-arenes in **3a**−**c** correspond to the symmetry of the free ligands. In particular, the typical septet/dublet of an isopropyl group, quartet/triplet of an ethyl group, and triplet/triplet of a $(CH_2)_2$ group, respectivly, are present in the NMR spectra of **3a**−**c**.

The μ-arene ring protons give rise to a singlet (for **3b**) or two (**3a**) or one (**3c**), respectivly, multiplets. Likewise there are one CH and one C resonances in the μ-arene region of the carbon spectrum of **3b**, whereas three CH and one C resonances are detected for the μ-arenes of **3a** and **3c**.

The spectra of **3d** are more complicated. Five proton and six carbon (5 CH and 1 C) resonances are found for the cluster coordinated phenyl ring of the 1,1-diphenylethane ligand, in contrast to the free ligand.

In both the ^{1}H and ^{13}C NMR spectra only one sharp resonance is observed for the three Cp groups of **3a**−**d**. The presence of hydrido ligands on the metal clusters is immediately obvious from the high-field resonances ($\delta \sim -14$) in the proton spectra. Compared to the starting materials **1a**−**d**, most affected by the protonation are the ^{1}H resonances of the Cp ligands, which are shifted to low field by $\Delta\delta = 0.5-0.8$. The resonances of the μ-arene ring hydrogens and those of the protons on C-α also experience a low-field shift but to a much lesser extent ($\Delta\delta = 0.1-0.3$). The ^{13}C NMR spectra of **1** and **3** are quite similar; only the resonances of the μ-arene *ipso* carbon atoms are notably shifted downfield ($\Delta\delta = 8-16$).

Variable-temperature NMR spectroscopic investigations were carried out with **3a**,**b**,**d**. Distinct changes of the spectra (especially the proton spectra) take place on lowering of the temperature. In **3a**, all proton resonances except the hydride signal and that of the methyne proton broaden. A similar effect is observed for **3b**, where only the hydride resonance remains unaffected. Unfortunately, limiting spectra could not be obtained due to the limited solubility of these salts below 230 K. Complex **3d** shows three sharp singlets for the Cp groups ($\delta = 5.38$, 5.40, and 5.46) in the proton spectrum at 230 K; of the three expected ^{13}C resonances for these ligands two accidentally coincide (Tables 1 and 2). Apart from minor changes in chemical shifts the resonances of the other protons and carbons in **3d** are identical at room temperature and 230 K.

(b) Crystal and Molecular Structure of [H(CpCo)$_3$(μ_3-η^2:η^2:η^2-1,1-diphenylethane)]$^+$-[CF$_3$COO]$^-$·H$_2$O (3d[CF$_3$COO]$^-$·H$_2$O). Single crystals of **3d**[CF_3COO]$^-$·H_2O were obtained from an aqueous solution. Crystal details are given in the Experimental Section. The molecular structure of **3d** is shown in Figure 1. Important bond lengths and angles are given in Table 3.

The crystal structure consists of discrete cations **3b** packed together with isolated trifluoroacetate anions. There are no unusual cation anion contacts. One molecule of lattice water, which is involved in a hydrogen bridge to one of the oxygen atoms of the trifluoroacetate, was found to be present in the asymmetric unit. The 1,1-diphenylethane ligand of **3d** is coordinated to the $(CpCo)_3$ triangle in the μ_3-η^2:η^2:η^2 fashion via one of its phenyl rings (Figure 1). The μ_3-arene is rotated by a few degrees within the plane parallel to the Co_3 triangle, away from the idealized staggered arrangement. As a consequence, the distances between each cobalt atom and the two μ-arene carbon atoms bonded to it are not equal (mean difference 0.07 Å). Endocyclic carbon carbon bond lengths within the μ_3-arene average 1.41 Å for the bonds located "on top" of the cobalt atoms and 1.44 Å for the others. All substituents are bent away from the metal cluster (displacements from the best plane through C(1)−C(6) are 0.54 Å for C(7) and 0.1−0.4 Å for the ring hydrogens). The arrangement

Table 1. ^{1}H NMR Data (200 MHz, δ at Ambient Temperature Unless Indicated Otherwise) for the Complexes $[(CpCo)_3\{\mu_3\text{-}R^3C_6H_4C(H)(R^1)(R^2)\}]$ (1a−d) and Their Protonation Products $[H(CpCo)_3\{\mu_3\text{-}R^3C_6H_4C(H)(R^1)(R^2)\}]^+$ (3a−d)

complex	hydride	Cp	μ-$C_6H_4R^3$	side chain [C(H)(R^1)(R^2)]
3a[a,b]	−14.4	5.30	4.29 ("t", 2H), 4.50−4.72 (m, 3H)	2.39 (sept, 1H, CH), 1.07 (d, 6H, CH_3)
1a[c,d]		4.72	4.20 ("t", 2H), 4.4 (m, 3H)	2.15 (sept, 1H, CH), 1.09 (d, 6H, CH_3)
3b[a,b]	−14.2	5.19	4.40 (s, 4H)	2.12 (q, 4H, CH_2), 1.05 (t, 6H, CH_3)
1b[c]		4.71	4.24 (s, 4H)	1.82 (q, 4H, CH_2), 1.19 (t, 6H, CH_3)
3c[a,e]	−14.7	5.28	4.4 (m, 5H)	2.36 ("t", 2H, CH_2), 2.76 (t, 2H, CH_2), 7.1 (m, 5H, Ph)
1c[c,f]		4.68	4.2 (m, 5H)	2.24 ("t", 2H, CH_2), 2.98 (t, 2H, CH_2), 7.2 (m, 5H, Ph)
3d[a,g]	−14.1	5.50	4.40 (t, 1H), 4.41 (t, 1H), 4.65 (t, 1H), 4.90 (d, 1H, *o*-H), 5.04 (d, 1H, *o*-H)	3.70 (q, 1H, CH), 1.41 (d, 3H, CH_3), 7.34 (m, 5H, Ph)
3d[a,e,h]	−14.1	5.38, 5.40, 5.46	4.26−4.36 (2t, 2H), 4.57 (t, 1H), 4.65 (d, 1H, *o*-H), 4.79 (d, 1H, *o*-H)	3.50 (q, 1H, CH), 1.34 (d, 3H, CH_3), 7.1−7.3 (m, 5H, Ph)
1d[c,d]		4.72	4.21 (m, 3H), 4.53 (d, 1H, *o*-H), 4.61 (d, 1H, *o*-H)	3.41 (q, 1H, CH), 1.25 (d, 3H, CH_3), 7.13 (m, Ph),[i] 7.30 (t, 2H, Ph), 7.47 (d, 2H, Ph)

[a] CF_3COO^- salt. [b] In CD_2Cl_2. [c] In C_6D_6. [d] 333 K. [e] In $CDCl_3$. [f] 313 K. [g] 300 MHz, in D_2O. [h] 230 K. [i] Overlap with solvent resonance.

Table 2. ^{13}C NMR Data (δ at Ambient Temperature Unless Indicated Otherwise) for the Complexes $[(CpCo)_3\{\mu_3\text{-}R^3C_6H_4C(H)(R^1)(R^2)\}]$ (1a−d) and Their Protonation Products $[H(CpCo)_3\{\mu_3\text{-}R^3C_6H_4C(H)(R^1)(R^2)\}]^+$ (3a−d)

complex	Cp	μ-$C_6H_4R^3$	side chain [C(H)(R^1)(R^2)]
3a[a,b]	83.6	43.2,[c] 43.9,[c] 44.6,[c] 79.3 (C-*ipso*)	37.8 (C-α),[c] 24.2 (CH_3)
1a[d]	82.5	39.8,[c] 40.8,[c] 41.9,[c] 63.5 (C-*ipso*)	38.6 (C-α),[c] 24.0 (CH_3)
3b[a,b]	83.9	45.5, 72.4 (C-*ipso*)	34.0 (CH_2), 17.7 (CH_3)
1b[d]	82.8	42.8, 63.5 (C-*ipso*)	35.0 (CH_2), 16.8 (CH_3)
3c[a,e]	83.6	42.5, 43.5, 46.9, 68.6 (C-*ipso*)	42.5 (CH_2), 43.7 (CH_2), 126.3 (Ph), 128.5 (Ph), 128.6 (Ph), 140.7 (Ph C-*ipso*)
1c[d,f]	82.5	39.3, 40.5, 44.6, 60.7 (C-*ipso*)	39.7 (CH_2), 43.5 (CH_2), 126.1 (Ph), 128.6 (Ph), 129.0 (Ph), 142.8 (Ph C-*ipso*)
3d[a,e]	83.7	42.3,[g] 42.6,[g] 43.9,[g] 46.4,[g] 47.8,[g] 74.6 (C-*ipso*)	43.2 (CH),[g] 20.8 (CH_3), 126.6 (Ph), 126.7 (Ph), 128.7 (Ph), 146.1 (Ph C-*ipso*)
3d[a,e,h]	83.2, 83.5	41.6,[g] 41.9,[g] 42.3,[g] 45.7,[g] 47.5,[g] 73.6 (C-*ipso*)	43.2 (CH),[g] 20.2 (CH_3), 126.3 (Ph), 126.6 (Ph), 128.5 (Ph), 145.8 (Ph C-*ipso*)
1d[d]	82.6	39.0,[g] 39.5,[g] 41.0,[g] 41.3,[g] 49.3,[g] 65.9 (C-*ipso*)	45.0 (CH),[g] 21.1 (CH_3), 126.2 (Ph), 127.4 (Ph), 128.6 (Ph), 149.2 (Ph C-*ipso*)

[a] CF_3COO^- salt. [b] In CD_2Cl_2. [c] CH, tentative assignment to μ-arene or C-α. [d] In C_6D_6. [e] In $CDCl_3$. [f] 313 K. [g] CH, μ-arene or C-α. [h] 220 K.

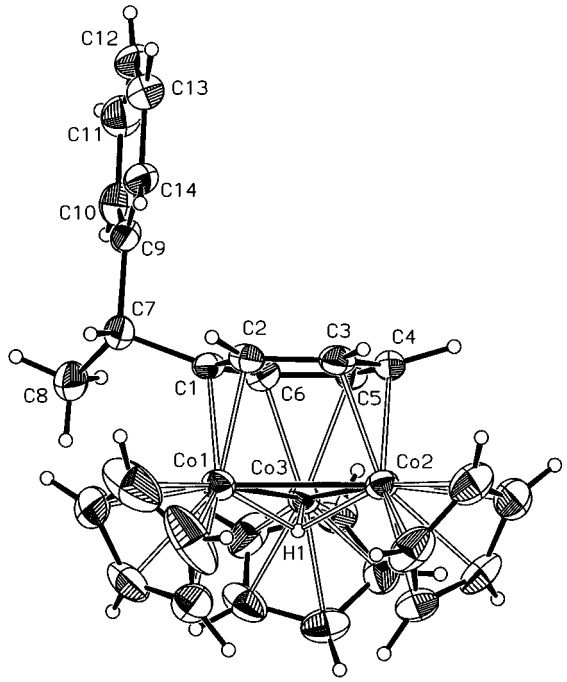

Figure 1. Molecular structure of **3d** in the crystal of **3d**$[CF_3COO^-]\cdot H_2O$.

Table 3. Selected Bond Lengths (Å) and Angles (deg) for 3d with Estimated Standard Deviations in Parentheses

Co(1)−Co(2)	2.589(2)	Co(1)−Co(3)	2.630(2)
Co(2)−Co(3)	2.593(2)		
Co(1)−C(1)	2.144(6)	Co(1)−C(2)	2.035(6)
Co(1)−C(Cp)[a]	2.063(1)−2.083(9)		
Co(2)−C(3)	2.084(7)	Co(2)−C(4)	2.038(6)
Co(2)−C(Cp)[a]	2.055(7)−2.106(8)		
Co(3)−C(5)	2.079(6)	Co(3)−C(6)	2.030(6)
Co(3)−C(Cp)[a]	2.069(8)−2.087(7)		
C(1)−C(2)	1.422(9)	C(1)−C(6)	1.452(9)
C(1)−C(7)	1.529(9)		
C(2)−C(3)	1.444(10)	C(3)−C(4)	1.402(10)
C(4)−C(5)	1.431(9)	C(5)−C(6)	1.409(9)
C(7)−C(8)	1.523(9)	C(7)−C(9)	1.542(9)
C(9)−C(10)	1.397(10)	C(9)−C(14)	1.377(9)
C(10)−C(11)	1.382(12)	C(11)−C(12)	1.343(12)
C(12)−C(13)	1.379(12)	C(13)−C(14)	1.373(10)
Co(1)−H(1)	1.63(5)	Co(2)−H(1)	1.70(5)
Co(3)−H(1)	1.57(5)		
Co(2)−Co(1)−Co(3)	59.56(5)	Co(1)−Co(2)−Co(3)	61.01(4)
Co(2)−Co(3)−Co(1)	59.43(5)		
C(2)−C(1)−C(6)	118.3(6)	C(2)−C(1)−C(7)	120.8(6)
C(6)−C(1)−C(7)	117.0(6)	C(1)−C(2)−C(3)	119.1(6)
C(4)−C(3)−C(2)	122.2(7)	C(3)−C(4)−C(5)	118.8(6)
C(6)−C(5)−C(4)	120.1(6)	C(5)−C(6)−C(1)	121.4(6)
C(8)−C(7)−C(1)	114.1(6)	C(8)−C(7)−C(9)	111.9(6)
C(1)−C(7)−C(9)	107.9(5)		

[a] C(Cp) denotes the carbon atoms of the cyclopentadienyl rings.

of the residues bonded to the α-carbon atom C(7) is such that the phenyl group points away from the $(CpCo)_3$ cluster, the methyl group in between Co(1) and Co(3), and the hydrogen atom in the direction of Co(1).

The hydrido ligand H(1) was located 0.64 Å above the Co_3 face which is not occupied by the arene ligand. The normals of the Cp ligands are at angles of 126.1(3), 125.7(2), and 124.0(3)° to the Co_3 plane.

Table 4. ^{1}H NMR Data (200 MHz, δ at Ambient Temperature) for the Complexes $[(CpCo)_3\{\mu_3\text{-}R^3C_6H_4C(R^2)=C(H)(R^1)\}]$ (2a−c) and Their Protonation Products $[(CpCo)_3\{\mu_3\text{-}R^3C_6H_4C(R^2)(CH_2R^1)\}]^+$ (4a−c)

complex	Cp	μ-$C_6H_4R^3$	side chain $[C(R^2)(CH_2R^1)]$
4a[a,b]	5.04 (10 H), 5.24 (5H)	3.58 (dd, 2H, H-1/5), 5.32 (tt, 1H, H-3), 5.81 (dd, 2H, H-2/4)	1.44 (s, 6H)
2a[b]	4.84[c,d]	4.46 (m, 3H), 4.84[c,d]	4.59 (dq, 1H, =CH), 5.07 (dq, 1H, =CH), 1.77 (dd, 3H, CH_3)
4b[b,e]	4.85 (5H),[c,f] 4.98 (5H), 5.29 (5H)	1.93 (dt, 1H), 4.67 (dt, 1H), 5.2 (m, 2H), 5.85 (td, 1H)	4.85 (m, CH),[c,f] 1.3 (m, CH_2),[c,g] 1.24 (dd, CH_3),[c,f] 0.9 (m, CH_2)
2b[h]	4.58 (15H)	4.2 (m, 3H), 4.4 (m, 2H)	5.44 (dq, 1H, =CH), 5.76 (dq, 1H, =CH), 1.57 (dd, 3H, CH_3)
4c[a,b]	5.09 (5H), 5.15 (5H), 5.36 (5H)[c,f]	1.45 (dd, 1H), 4.16 (dd, 1H), 5.34 (m),[c,f] 6.31 (dd, 1H), 3.69 (s, 3H, OCH_3)	5.42 (q, 1H, CH), 1.36 (d, 3H, CH_3)
2c[i]	4.67 (15H)	4.18 (m, 2H),[j] 4.55 (m, 2H),[j] 3.00 (s, 3H, OCH_3)	6.09 (dd, 1H, CH), 4.83 (dd, 1H, CH), 5.10 (dd, 1H, CH)

[a] CF_3COO^- salt. [b] In CD_2Cl_2. [c] Overlapping peaks. [d] Total intensity 17 H. [e] BPh_4^- salt. [f] Total intensity 16H. [g] Total intensity 4H. [h] In toluene-d_8. [i] In C_6D_6. [j] $(AB)_2$ system.

Table 5. ^{13}C NMR Data (δ at Ambient Temperature) for the Complexes $[(CpCo)_3\{\mu_3\text{-}R^3C_6H_4C(R^2)=C(H)(R^1)\}]$ (2a−c) and Their Protonation Products $[(CpCo)_3\{\mu_3\text{-}R^3C_6H_4C(R^2)(CH_2R^1)\}]^+$ (4a−c)

complex	Cp	μ-$C_6H_4R^3$	side chain $[C(R^2)(CH_2R^1)]$
4a[a,b]	84.4, 87.3	38.0, 50.2, 51.1, 81.4 (C-*ipso*)[c]	105.6 (C),[c] 27.3 (CH_3)
2a[d]	82.6	39.6, 40.1, 41.1, 59.3 (C-*ipso*)	149.8 (C-α), 104.7 (=CH_2), 21.7 (CH_3)
4b[b,e]	83.4, 84.6, 86.1	37.3,[c] 41.5,[c] 50.2,[c] 51.3,[c] 129.2 (C-*ipso*)[c]	80.0 (C-α),[c] 25.7 (CH_2), 15.3 (CH_3)
2b[f]	82.7	39.2, 40.9, 41.8, 56.1 (C-*ipso*)	116.4 (=CH), 140.1 (=CH), 16.4 (CH_3)
4c[a,b]	84.1, 84.8, 85.8	32.8 (CH), 33.0 (CH), 40.8 (CH), 41.8 (CH), 79.5 (C), 120.5 (C), 56.7 (OCH_3)	76.3 (C-α), 18.0 (CH_3)
2c[f]	83.8	33.1, 38.4, 49.3 (C), 53.7 (C), 55.7 (C), 55.7 (OCH_3)	145.7 (=CH), 104.3 (=CH_2)

[a] CF_3COO^- salt. [b] In CD_2Cl_2. [c] Tentative assignment. [d] In toluene-d_8. [e] BPh_4^- salt. [f] In C_6D_6.

(B) Protonation of the Cluster Complexes $[(CpCo)_3(\mu_3\text{-}R^3C_6H_4\{C(R^2)=CHR^1)\}]$ (2a−c). (a) Syntheses and Spectra. With trifluoracetic acid (molar ratio 1:1 or excess of acid) in dichloromethane the complexes **2a**−**c** are protonated on the β-carbon atom of the unsaturated side chain on the μ_3-arene. When the protonations were carried out in CD_2Cl_2 in an NMR tube, complete conversion to the products **4** was observed within a few seconds at room temperature. In a preparative scale, the trifluoroacetates were obtained as air-sensitive dark brown oils, which are soluble in dichloromethane or thf, less so in water, and unsoluble in toluene or petroleum ether. As with **3**, the trifluoroacetates of **4b**,**c** may be subjected to salt metathesis to give the black microcrystalline tetraphenylborates **4b**$[BPh_4]^-$ and **4c**$[BPh_4]^-$ in about 40% yield. Only the parent ions **4a**−**c** are found in the field desorption positive ion mass spectra of both the CF_3COO^- and BPh_4^- salts.

When an aqueous solution of **4a**$[CF_3COO]^-$ was layered with Et_2O and then treated with excess sodium bicarbonate, the aqueous phase became colorless within a few hours. The neutral cluster complex **2a** was present in the ether phase. Solutions of **4a**$[CF_3COO]^-$ in dichloromethane slowly decomposed, even at low temperature. After 3 weeks at −20 °C a small amount of dark precipitate formed, and no **4a** could be detected any more. By NMR analysis, an about 3:1 mixture of **2a** and its hydrogenation product, **1a**, was found in the supernatant solution.

Likewise, **1a** is also formed in variable amounts when **4a**$[CF_3COO]^-$ is allowed to stand for prolonged periods in aqueous or methanol solutions.

^{1}H and ^{13}C NMR spectroscopic data for **4a**−**c** are given in Tables 4 and 5. The spectra are dissimilar from those of the starting materials **2a**−**c** and are independent of temperature within the range 200−340 K. In the proton and carbon spectra two resonances are found for the CpCo groups of **4a**, whereas three such resonances are present in the spectra of **4b**,**c**. Compared to the neutral starting materials, the ^{1}H resonances are shifted downfield by 0.2−0.7 ppm. The shifts of the Cp carbon atoms are not much affected by the protonation.

Unlike in the starting material, only three multiplets (intensity ratio 2:1:2) and one methyl resonance (intensity 6) are due to the bridging ligand in the ^{1}H NMR spectrum of **4a**. A similarly reduced number of resonances (three CH, two C, and one CH_3) are detected for this ligand in the carbon spectrum. In contrast, separate ^{1}H and ^{13}C resonances appear for every single C, CH_2, and CH_3 group in **4b**,**c**.

The multiplets of the ring protons of the bridging ligands are unusually far apart from one another on the δ-scale (**4a**, $5.81 \geq \delta \geq 3.58$; **4b**, $5.85 \geq \delta \geq 1.93$; **4c**, $6.31 \geq \delta \geq 1.45$). Series of homonuclear decoupling experiments were carried out with **4a**−**c**. The proton spectrum of **4a** could be completely assigned (Table 4). Coupling constants ^3J(HH) between the pairs of vicinal protons H-2/3 and H-3/4 are 6.6 and 6.3 Hz, respectively. The coupling between the 1,3 protons H-2/4 is much smaller, ^4J(HH) = 1.4 Hz.

In the much more complicated case of **4c** there are two pairs of strongly (^3J(HH) = 6.8 Hz) coupled protons (δ = 1.45/6.31 and δ = 4.16/5.34). These are connected with each other by weaker couplings (J(HH) = 2.2 Hz) [δ = 6.31 (dd) with δ = 5.34 (m), and δ = 4.16 (dd) with δ = 1.45 (dd)]. This set of four multiplets is assigned to the resonances of the ring CH groups of the bridging ligand. The proton on C-α (a quartet at δ = 5.42) is clearly identified by its coupling to the methyl group. The ^{1}H resonance of the methoxy group in **4c** is considerably shifted downfield compared to the starting material **2c** ($\Delta\delta$ = 0.69).

Similar chains of adjacent vicinal CH protons were established in the spectrum of **4b**. However, due to considerable overlap of signals, the connectivity matrix is not complete. Established assignments are $\delta = 1.93$ (dt, H-2), $\delta = 5.85$ (td, H-3) and $\delta = 4.67$ (dt, H-6). The resonance of the proton on C-α is partially obscured by one of the Cp peaks but could be identified by its coupling to the two diastereotopic methylene protons, which appear as separate multiplets (Table 4).

In the ^{13}C NMR spectra of **4a**−**c** low-field resonances due to olefinic CH or CH_2 groups are absent. The most interesting signals—those of the *ipso* and α-carbon atoms—could not in all cases be unambigously assigned. There is only one quaternary carbon (C-*ipso*) in **4b**, which resonates at $\delta = 129.2$. In **4a**, two such resonances (C-*ipso* and C-α) are detected at $\delta = 81.4$ and 105.6. There are two C-*ipso* in **4c**, consistent with the observed resonances at $\delta = 79.5$ and 120.5.

The resonances of the α-carbons are difficult to assign. In **4a**, there is a choice between $\delta = 81.4$ and $\delta = 105.6$, whereas in **4b**,**c** more possibilities exist. A tentative assignment is given in Table 5, which assumes a low-field shift for C-α.

(b) Attempted Synthesis of 4a[BPh$_4$]$^-$. Formation of [(CpCo)$_3$(μ_3-α-methylstyrene]$^+$[BPh$_4$]$^-$. In an attempt to crystallize **4a** as a tetraphenylborate salt, a dichloromethane solution of **4a**[CF_3COO]$^-$ was treated with $NaBPh_4$. After removal of a colorless precipitate, the mixture was layered with petroleum ether and cooled to −20 °C. Black crystals were formed from this solution within several days. The field desorption mass spectrum of these crystals gave a strong parent ion at $m/z = 490$ (**2a**$^+$). In the course of several days, a total yield of 20% **2a**$^+$[BPh_4]$^-$ was collected in several fractions.

The product was not stable in solution at room temperature. When a sample was dissolved in CD_2Cl_2 at −70 °C and transferred to the precooled (−40 °C) NMR probe, a proton spectrum with very broad strong peaks in the range $7 \geq \delta \geq -4.5$ was measured. When the sample was warmed above 270 K, the broad features began to change with time. After 24 h at room temperature, a well-resolved spectrum was observed, showing the resonances of **4a** (30%), **2a** (30%), BPh_4^-, and unidentified decomposition products (10%).

As expected, **2a**$^+$ could also be prepared directly by oxidation of **2a** with $AgBF_4$.

(c) Crystal and Molecular Structure of [(CpCo)$_3$(μ_3-η^2:η^2:η^2-α-methylstyrene)]$^+$[BPh$_4$]$^-$·0.5 CH$_2$Cl$_2$ (2a$^+$[BPh$_4$]$^-$·0.5 CH$_2$Cl$_2$). Three X-ray diffraction data sets were collected from three different crystals of rather poor quality. All data sets were solved to give the same gross structure, but only the set with the largest number of observed reflections was used for refinement. Details are given in the Experimental Section. The molecular structure of **2a**$^+$ is shown in Figure 2. Important bond lengths and angles are given in Table 6.

The structure consists of an array of cluster complex cations and BPh_4^- anions in a 1:1 ratio. Methylene chloride is present in the crystal as a solvent of crystallization. In the cation, a $(CpCo)_3$ triangle is capped in the μ_3-η^2:η^2:η^2 fashion by an essentially planar (max deviation 0.04 Å) arene ligand, which bears a branched three-carbon side chain. The configuration of the α-carbon atom C(7) is planar, with one longer (1.475(6) Å) bond to the *ipso* carbon C(1) and two shorter bonds of approximately equal length (1.403(8) Å and 1.413(8) Å) to the terminal carbon atoms C(8) and C(9). The plane defined by C(1), C(7), C(8), and C(9) is at an angle of 23.6(6)° to the μ_3-arene. The coordination of the latter to the Co_3 triangle is somewhat asymmetric. As in **3d**, the C_6 ring is rotated in the plane parallel to the Co_3 triangle away from the staggered arrangement, resulting in a mean difference in length of 0.14 Å between the two Co−C(C_6) bonds of every cobalt atom. Taking in account the relatively large errors, there is no pronounced carbon carbon bond length alternation within the μ_3 arene ring. However, all taken together, the carbon−carbon bonds "on top" of the metal atoms are slightly shorter (difference between the arithmetic means, 0.01 Å).

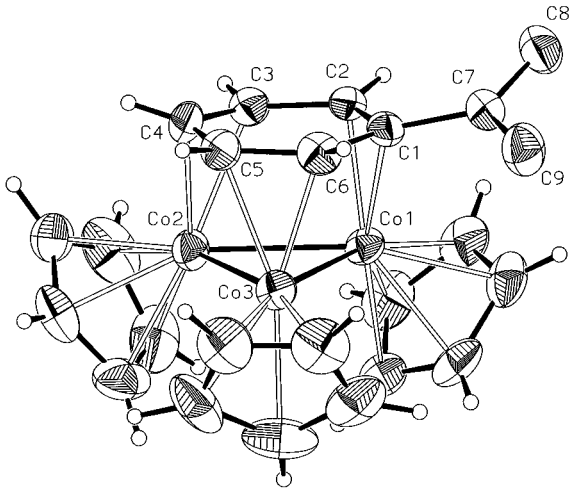

Figure 2. Molecular structure of **2a**$^+$ in the crystal of **2a**$^+$[BPh_4^-]·CH_2Cl_2. Hydrogen atoms on the side chain are not shown.

Table 6. Selected Bond Lengths (Å) and Angles (deg) for 2a$^+$ with Estimated Standard Deviations in Parentheses

Co(1)−Co(2)	2.4564(13)	Co(2)−Co(3)	2.4249(14)
Co(1)−Co(3)	2.4939(14)		
Co(1)−C(1)	2.174(4)	Co(1)−C(2)	1.999(5)
Co(1)−C(Cp)[a]	2.061(5)−2.123(5)		
Co(2)−C(3)	2.159(5)	Co(2)−C(4)	1.999(6)
Co(2)−C(Cp)[a]	2.084(6)−2.121(6)		
Co(3)−C(5)	2.104(5)	Co(3)−C(6)	2.018(5)
Co(3)−C(Cp)[a]	2.071(6)−2.138(6)		
C(1)−C(2)	1.413(7)	C(1)−C(6)	1.425(7)
C(1)−C(7)	1.475(6)	C(2)−C(3)	1.412(7)
C(3)−C(4)	1.397(8)	C(4)−C(5)	1.410(8)
C(5)−C(6)	1.407(7)	C(7)−C(8)	1.413(8)
C(7)−C(9)	1.403(8)		

Co(2)−Co(1)−Co(3)	58.66(4)	Co(3)−Co(2)−Co(1)	61.44(3)
Co(2)−Co(3)−Co(1)	59.90(3)		
C(2)−C(1)−C(6)	116.8(5)	C(2)−C(1)−C(7)	121.9(4)
C(6)−C(1)−C(7)	119.9(5)	C(3)−C(2)−C(1)	121.1(5)
C(4)−C(3)−C(2)	120.5(6)	C(3)−C(4)−C(5)	119.4(5)
C(6)−C(5)−C(4)	119.2(5)	C(5)−C(6)−C(1)	122.3(5)
C(9)−C(7)−C(8)	120.9(6)	C(9)−C(7)−C(1)	120.0(5)
C(8)−C(7)−C(1)	119.1(5)		

[a] C(Cp) denotes the carbon atoms of the cyclopentadienyl rings.

(d) Reaction of [(CpCo)$_3$(μ_3-1,1-diphenylethene)] (2d) with CF$_3$COOH. An excess of CF_3COOH was added to a sample of **2d** in CD_2Cl_2 at room temperature. Proton spectra measured immediately after the addition of the acid showed very broad features in the region $4.7 > \delta > 3.7$, which changed with time and slowly became

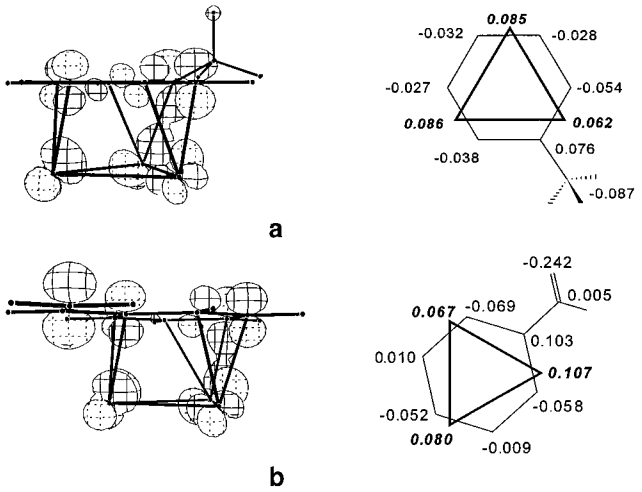

Figure 3. The HOMO (left side) and the charge distribution in the metal triangle and in the arene ligand (right side) for $[(CpCo)_3(C_6H_5CH_3)]$ (top) and $[(CpCo)_3\{C_6H_5(C(H)=CH_2)\}]$ (bottom). Cobalt charges are written in bold and italic type.

sharper. Other somewhat broadened resonances elsewhere in the spectrum (notably the methyl resonance at $\delta = 1.28$) could be assigned to the hydrogenation product of **2d**, i.e. $[(CpCo)_3(\mu_3\text{-}1,1\text{-diphenylethane})]$ (**1d**). In addition, the resonances of free 1,1-diphenylethane were also present in the spectra from the very beginning. The signals due to these latter two products grew more intense with time. There were two more resonances, a quintetlike signal at $\delta = 3.00$ and two multiplets at $\delta = 6.48, 6.58$ (intensity ratio about 1:1:1), which showed spin−spin coupling to each other. After about 24 h, all resonances were sharp. Apart from the three last mentioned multiplets all signals could be assigned to **1d** (about 70% of the total intensity) and 1,1-diphenylethane (about 25%).

A second reaction carried out with less than the stoichiometric amount of acid showed similar results, except that residual **2d** could be detected throughout the reaction. When this reaction mixture was taken to dryness after several days and then treated with C_6D_6, the only proton resonances in the benzene extract were those of **2d** (35%), **1d** (35%), and 1,1-diphenylethane (30%).

(C) Molecular Orbital Calculations. Model complexes containing the cluster frame $(CpCo)_3$ and simple arene ligands with the minimum amount of substituents needed to define the type of ligand were used (further details may be found in the Experimental Section).

(a) Site of Protonation of the Clusters. As described above, clusters **1** and **2** exhibit different behavior toward protonation. Calculations were performed for two typical models, namely, $[(CpCo)_3(\mu_3\text{-}C_6H_5CH_3)]$ (**1′**) (as a model for **1**) and $[(CpCo)_3\{\mu_3\text{-}C_6H_5(C(H)=CH_2)\}]$ (**2′**) (as a model for **2**). After optimization of the orientation of the arene relative to the Co_3 triangle, the HOMOs for the two clusters and the more relevant charges were analyzed to try and understand the protonation reactions. A three-dimensional picture of each HOMO, and a scheme of the geometry containing some atomic charges are shown in Figure 3.

The HOMO is much more localized on the cobalt atoms for **1′** (49.3% compared to 39.3% in **2′**), while a strong contribution from the β carbon appears in **2′**. The cobalt atoms carry charges close to zero and slightly smaller for **1′**; the largest negative charge in **2′** is by far that of the β carbon.

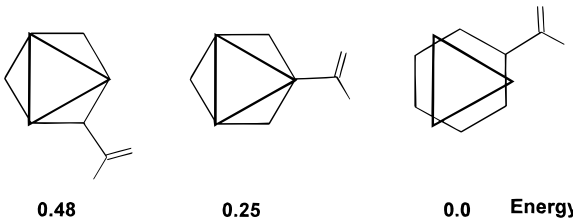

Figure 4. The relative energies of the staggered and the two eclipsed geometries of $[(CpCo)_3\{C_6H_5(C(H)=CH_2)\}]^+$.

(b) Structure of $2a^+$. The structural preferences of the paramagnetic cation were analyzed. Starting from $[(CpCo)_3\{\mu_3\text{-}C_6H_5(C(H)=CH_2)\}]^+$, the planar arene ligand was allowed to rotate relative to the triangular cluster. The preferred conformation is obtained when the arene is rotated 12° away from the staggered geometry, as it allows for minimal steric repulsion between the cyclopentadienyl groups and the substituent (Figure 4). The situation repeats every 120°. In $[(CpCo)_3\{\mu_3\text{-}C_6H_5(C(Me)=CH_2)\}]^+$, where the proton on C-α was replaced by a methyl group, the potential energy surface is steeper and the deviation from the staggered geometry larger (30°).

The effect of bending the side chain away from the arene plane was then studied. The hydrogen atoms were kept in the plane, although they are also bent in the experimental structures, because this allowed us to isolate the effect of the side chain. The energy became lower (close to 1 eV) when the side chain was bent by ca. 15° for $[(CpCo)_3\{\mu_3\text{-}C_6H_5(C(H)=CH_2)\}]^+$ and ca. 20° for $[(CpCo)_3\{\mu_3\text{-}C_6H_5(C(Me)=CH_2)\}]^+$. The minima are rather soft within 5−10°.

(c) Structure of the Protonated Derivatives 4. For simplicity, $[(CpCo)_3(\mu_3\text{-}C_6H_5CH_2)]^+$ was used as a model for **4**, as the important aspects of the bonding between the cobalt triangle and the arene will be kept. The arene ligand was rotated over the cobalt triangle, in order to find their preferred relative orientation.

The staggered geometry is the most favorable, as in the case of benzene. In order to find alternative coordination modes, the arene was allowed to slip in the plane parallel to the Co_3 triangle, starting from an eclipsed structure. The Walsh diagram in Figure 5 shows a minimum of the total energy for a slipping of 0.7 Å. The energy for this geometry is comparable (0.009 eV higher) to that of the most stable form above (staggered), although it has not yet been optimized.

The lowering of total energy as the slipping distortion proceeds is reflected by molecular levels such as the second highest occupied molecular orbital, which starts as antibonding between cobalt and the side chain carbon and becomes bonding [Co−(C-α) overlap population goes from 0.032 to 0.181 at the minimum energy], as seen in Figure 6. On the other hand, a fragment analysis indicates the increased participation of π orbitals containing large percentages of the side chain carbon in the bonding.

We tried to optimize the bending of the side chain for the previous slipped geometry. The potential energy is relatively soft around a minumum at 190° (i.e. away from the Co_3 cluster by 10°).

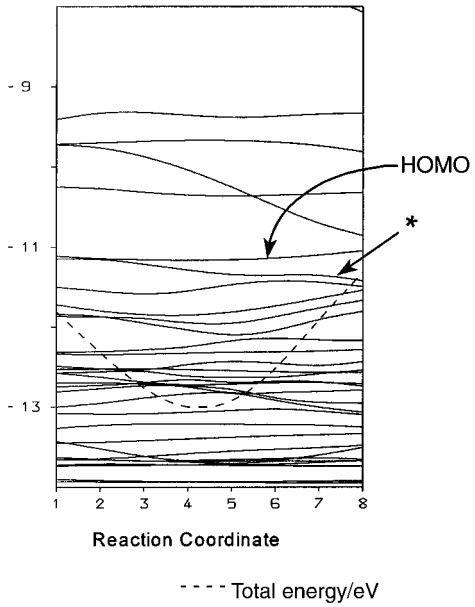

Figure 5. Walsh diagram for slipping the benzyl cation $C_6H_5CH_2^+$ across the Co_3 triangle. Between steps on the reaction coordinate the slipping is increased by 0.2 Å. The orbital shown in Figure 6 is marked by an asterisk (*).

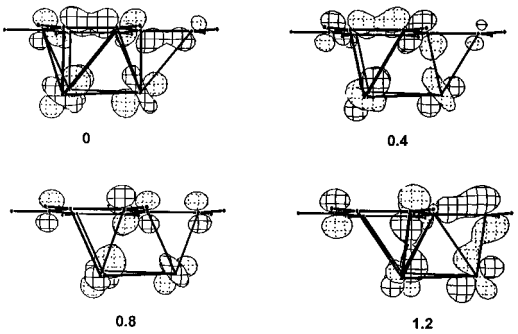

Figure 6. Second highest occupied molecular orbital when the arene ligand has slipped 0, 0.4, 0.8, and 1.2 Å.

The slipping motion, where the carbon atoms of the side chain approach one cobalt, also results in moving the *para*-carbon atom of the arene away from the two other cobalt atoms. The best geometry should be one which optimized all the carbon−cobalt distances, including the slipping distortion and the bending of the arene, allowing the side chain carbon to approach one cobalt and the *para*-carbon to approach the other two cobalts.

In order to obtain a more reliable geometry for the cation, this optimization was done using density functional calculations (ADF program).

The final optimized geometry is shown in Figure 7a, while the Co_3 triangle and the arene are shown in more detail in Figure 7b,c (top and side views, respectively). This geometry is similar to the one obtained by the extended Hückel method in that the arene is slipped and the side chain bent upward, away from the metal cluster. Also, the carbon *para* to the side chain is bent toward two cobalt atoms of the cluster, in order to allow for a shorter cobalt−carbon distance.

Discussion

(A) Hydrido Cluster Cations $[H(CpCo)_3\{\mu_3\text{-}R^3C_6H_4C(H)(R^1)(R^2)\}]^+$ (3a−d). The variable-temperature NMR spectra of the protonated complexes **3a**−**d** are quite similar to those of their neutral precursors **1a**−**d**. Hence we can conclude that the solution structures of the two series of cluster complexes must be closely related. The presence of resonances in the high-field region of the ^1H NMR spectra clearly shows that protonation of **1a**−**d** takes place at the metal framework. Integration of the ^1H NMR spectra, and field desorption mass spectra, consistently indicates that monohydrido cations are formed. Protonation of **1** at the metal cluster may be rationalized using charge and overlap control arguments (*vide infra*).

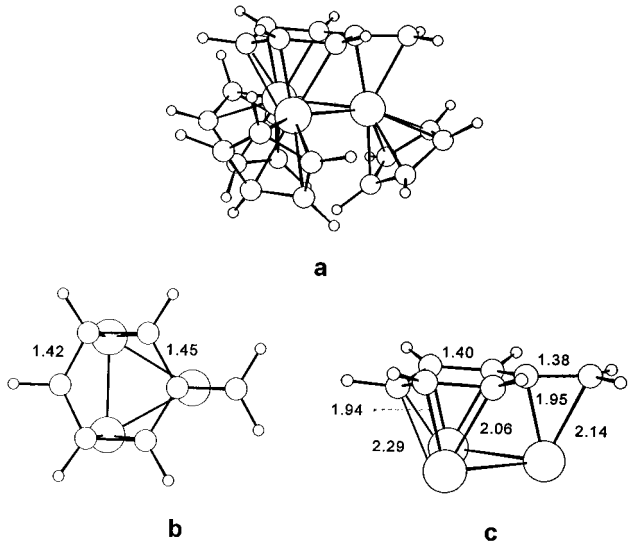

Figure 7. Optimized geometry of $[(CpCo)_3(\mu\text{-}C_6H_5CH_2)]^+$: complete molecule (side view, a); top view omitting the Cp ligands (b); side view omitting the Cp ligands (c). Relevant bond distances are given in Å.

Co_3 face-capping sites for the hydrido ligands are consistent with the highly symmetrical NMR spectra of **3a** at high temperature. However, fluxional Co_2 edge-bridging hydrides cannot be ruled out *a priori* on the basis of the observed NMR chemical shifts alone [$\delta(^1H)$ around −15]. These are fairly low compared to those of other cationic or even neutral hydrido cluster complexes with $(CpCo)_n$ cores, e.g. $[(\mu_2\text{-}H)(CpCo)_3(CCH_3)_2]^+$ ($\delta(^1H) = -26.4$) or $[(\mu_3\text{-}H)_n(CpCo)_4(CCH_3)]^{(n-1)+}$ ($n = 1$, $\delta(^1H) = -19.6$; $n = 2$, $\delta(^1H) = -22.1$; $n = 3$, $\delta(^1H) = -25.2$),[9] and come closer to the μ_2- ($\delta = -12$) than to the μ_3-hydride resonance ($\delta = -28$) in the neutral dihydrido cluster complexes $[(\mu_2\text{-}H)(\mu_3\text{-}H)(CpCo)_3(\mu\text{-}\eta^1\text{:}\eta^2\text{:}\eta^1\text{-alkyne})]$.[10] For crystalline **3d**$[CF_3COO]^-$ a face-capping μ_3-hydride was established by X-ray crystallography (*vide supra*). We believe that this type of hydride coordination is also retained in solution for steric reasons.

The gross geometry of the $(CpCo)_3(\mu_3\text{-arene})$ cluster unit in **3d** nicely matches that of many other neutral (non-protonated) complexes of this type.[3,11,12] However, the $(CpCo)_3(\mu_3\text{-arene})$ moiety is expanded compared to

(9) Wadepohl, H.; Pritzkow, H. *J. Organomet. Chem.* **1993**, *450*, 9.
(10) (a) Wadepohl, H.; Borchert, T.; Büchner, K.; Pritzkow, H. *Chem. Ber.* **1993**, *126*, 1615. (b) Wadepohl, H.; Borchert, T.; Pritzkow, H. *J. Chem. Soc., Chem. Commun.* **1995**, 1447. (c) Wadepohl, H.; Borchert, T.; Pritzkow, H. *Chem. Ber.*, in press.
(11) Wadepohl, H. In *The Synergy Between Dynamics and Reactivity at Clusters and Surfaces*; Farrugia, L. J., Ed.; Nato ASI Series C: Mathematical and Physical Sciences, Vol. 465; Kluwer, Dordrecht, 1995; p 175.
(12) Wadepohl, H.; Gebert, S. *Coord. Chem. Rev.* **1995**, *143*, 535.

1d. This affects mainly the cobalt−cobalt bonds (2.604 Å (av) in **3d** vs 2.504 Å (av) in **1d**), but the distances from the cobalt atoms to the μ_3-arene are also somewhat longer in **3d** (d[Co−C(μ-arene)]$_{av}$ = 2.068 Å (**3d**) vs 2.034 Å (**1d**)). Quite significantly, the coordination geometry of the μ_3-arene ligand with respect to the Co_3 triangle in **1d** more closely approaches an ideal staggered arrangement than it does in **3d**, where particularly C(1) is shifted away from Co(1). In addition, the Cp ligands are bent "upward" in the direction of the μ_3-arene by about 5° relative to their position in **1d**. These geometrical differences indicate a considerable steric congestion around the Co_3 core in **3d**, which is caused by the additional spatial requirements imposed on the cluster by the hydrido ligand.

The other geometrical parameters of the μ_3-arene in **3d**—notably the expansion and (barely significant) alternation in length of the endocyclic carbon carbon bonds and the displacement of the substituents from the ring plane away from the metal cluster—are well within the range usually found in this class of compounds.[3,7,8,11,12]

The temperature dependence of the NMR spectra is characteristic of a hindered rotation of the μ_3-arene ligands on top of the Co_3 clusters.[3,11] Depending on the symmetry of the arene, different stereochemical situations arise. These dynamic processes will be dealt with in more detail in a forthcoming paper.[13] Here we shall only briefly discuss the salient features of the relevant systems.

Of the molecules to be described here, **3b** represents the most simple case. In the ground state with a staggered arrangement of C_6 and Co_3 rings, a plane of symmetry relates the two ethyl groups, two pairs of arene ring CH groups, and two of the three Cp ligands. Hence, a very simple carbon spectrum is observed at low temperature (two resonances due to the ethyl groups, two ring CH, and two Cp resonances). However, the proton spectrum is more complicated. Due to the prochiral nature of the ethyl groups, the two methylene hydrogens become diastereotopic, which should result in the observation of an ABX_3 type spin system for the ethyl groups at low temperature. When the temperature is increased, arene rotation becomes fast on the NMR time scale; this averages the anisochroneous methylene hydrogens. As a consequence, the ordinary ethyl pattern (quartet/triplet) is expected at high temperature. Such a temperature dependence of the proton spectra is indeed observed for the neutral complex **1b**. However, the limited solubility of **3b**$[CF_3COO]^-$ prevented NMR spectroscopic investigations below 230 K; at this temperature, μ_3-arene rotation is still fast enough to substantially broaden the Cp and CH_2 resonances.[14]

The complexes **3a**,**c** have less symmetrical ligands. Consistent with rapid μ_3-arene ring rotation only four ^{13}C NMR resonances (three CH and one C) are detected at high temperature for the μ_3-arene ring carbon atoms. The temperature dependence of the proton spectrum of **3a** is as expected for a slowdown of the dynamic process with decreasing temperature.[14] The broadening of the Cp and methyl resonances indicates that these groups become anisochroneous at low temperature, which is what is expected for a static (on the NMR time scale) structure.

Due to the presence of an asymmetric α-carbon atom, the stereochemical situation in **3d** (and also **1d**) is quite different. There are four nonequivalent possibilities to put the 1,1-diphenylethane ligand onto the $(CpCo)_3$ cluster in the μ_3-η^2:η^2:η^2 bonding mode. Using the same face of one arene to bind to the metal cluster, two chiral diastereomers can be generated, which differ by a 60° rotation of the μ_3-arene in the plane parallel to the Co_3 triangle.[3,11] The observation of only one resonance for the CpCo groups in the ^{1}H and ^{13}C NMR spectra, respectively, of **3d** (and also **1d**) shows that this isomerization is rapid at room temperature. Again, μ_3-arene rotation slows down when the temperature is lowered. However, only one set of three ^{1}H and two ^{13}C resonances (due to accidental degeneracy of two carbon signals) is found at 230 K. Therefore, only one of the two diastereomeric "rotamers" can be significantly populated at low temperature (the concentration of the other isomer is less than 5%, judging from the signal-to-noise ratio of the proton spectrum). This must be the result of a considerable difference in the free enthalpy of the isomers. With an estimated equilibrium constant $K \leq 0.05$, we calculate $\Delta G° \geq 6$ kJ·mol^{-1}.[15] This value represents the lower limit for the standard free reaction enthalpy $\Delta G°$ of the elementary step of arene rotation and is related to, but not equivalent, to the free enthalpy of activation for this process.[13]

A racemic mixture of only one of the two diastereomers is present in crystalline **3d**$[CF_3COO]^-$· As can be seen from Figure 1, this is the sterically least hindered arrangement of the μ_3-η^2:η^2:η^2 arene ligand. Therefore we believe that this structure also represents the ground state of **3d** in solution.

(B) Cations $[(CpCo)_3(\mu_3\text{-}R^3C_6H_4\{C(R^2)CH_2R^1\}]^+$ (4a-c). The NMR spectra of the protonation products **4a**−**c** are dissimilar from those of the neutral starting materials, the (1-alkenyl)benzene cluster complexes **2a**−**c**. On the basis of the general appearance and independence of temperature of the spectra, we can conclude that **4a**−**c** have rigid structures, which must be quite different from those of **2a**−**c**. Field desorption mass spectrometry, careful integration of the proton spectra, and the determination of the multiplicity of the carbon resonances prove that the products **4a**−**c** result from monoprotonation of **2a**−**c** on a carbon atom of the alkenyl side chains, in the position β to the μ_3-arene ring. However, the simplistic formulation **A** (Chart 2) of **4a**−**c** as cluster complexes with a μ_3-η^2:η^2:η^2 coordinated benzyl cation is in contradiction with the NMR data.

First, the possible carbon resonances for C-α are in the range $76 \leq \delta \leq 130$ and, thus, at a field much too high for carbocationic centers.[16]

Second, at least in **4a**, the bridging ligand must be coordinated to the metal cluster in a way which is more symmetrical than the μ_3-η^2:η^2:η^2 fashion. The number of ^{1}H and ^{13}C resonances of **4a** (only one methyl and three CH signals, along with two quaternary carbons)

(13) Wadepohl, H.; Herrmann, M.; Jost, C.; Müller, S. Manuscript in preparation.
(14) Jost, C. *Zulassungsarbeit*; Universität Heidelberg, 1995.
(15) Using $\Delta G° = -RT \ln(K)$ (van't Hoff reaction isotherm). $\Delta G°$ is the standard enthalpy of reaction for the conversion of the two isomers.
(16) Vogel, P. *Carbocation Chemistry*; Elsevier: Amsterdam, 1985; Chapter 4.

Chart 2

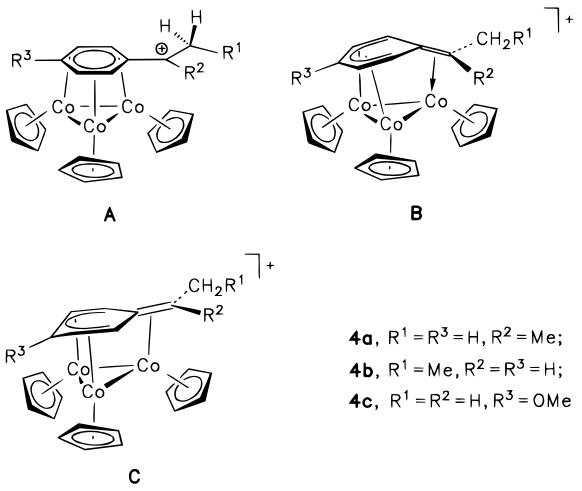

resemble the symmetry of the free α,α-dimethylbenzyl ligand. The presence of only two ^{1}H and ^{13}C resonances due to the CpCo groups of **4a** is also inconsistent with a staggered μ_3-η^2:η^2:η^2 arrangement.

On the basis of the above arguments, we previously proposed structure **B** for the cluster coordinated benzyl cations.[3] This is consistent with the mirror symmetry apparent in the ^{1}H and ^{13}C NMR spectra of **4a**. Since all of the C_6 ring carbons and C-α are metal coordinated, and the positive charge is highly delocalized, it also accounts for the lack of low-field carbon resonances. In addition, there were obvious parallels to the α-carbinyl-$[(CO)_3Co]_3$-substituted carbonium ions **5**[17] and related

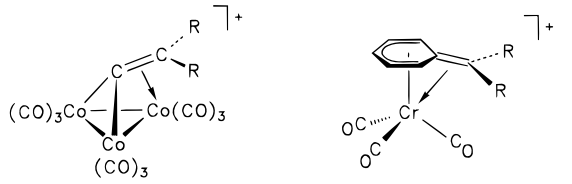

cluster-stabilized carbocations[18] as well as to the mononuclear $(CO)_3Cr$-stabilized benzyl cations **6**.[19] In all these cases, stabilization is achieved by coordination of the carbocationic center to a metal. Judged from the carbon NMR shifts, the interaction of C-α with the Co_3 cluster in **4** appears to be even stronger than that with the chromium in **6**. In one of the latter complexes, $[(CO)_3Cr(C_6H_5CMe_2)]^+$, C-α resonates at δ = 170.9, shielded by $\Delta\delta$ = 83 relative to the free ligand, viz., $[C_6H_5CMe_2]^+$.[20] The two possible resonances for C-α in **4a**, which has the same ligand, are much more shielded ($\Delta\delta$ = 148 and 173, respectively).

However, our MO calculations indicate that, although qualitatively correct with respect to the slip of the Co_3 triangle relative to the benzyl ligand and the strong interaction of the α-carbon atom with the Co_3 cluster, **B** is not the correct structure. The calculated energy minimum **C** differs in that the α-carbon atom bends away from instead of toward the metal cluster. In addition, the six-membered ring is folded to bring the carbon atom *para* to the benzylic side chain closer to the metal cluster (Figure 7). The results of our calculations are discussed in full detail in section D below.

The complexes **4b**,**c** are inherently less symmetrical than **4a**. In both complexes separate resonances are observed for the three CpCo groups, for all C_6 ring carbons, and all C_6 ring hydrogens. This would be consistent with structure **C** under the reasonable assumption that rotation of the protonated substituent around the bond (C-*ipso*)−(C-α) is prohibited.

However, the chemical shifts of the protons on the C_6 rings in **4b**,**c** fall into a much wider range than in **4a**. In particular, the pronounced high-field shift of one resonance (δ = 1.93 in **4b**, δ = 1.45 in **4c**) is hard to explain by a steric effect alone, caused by the two different substituents on C-α. It may therefore well be that the actual structure of these two derivatives is somewhat distorted from the ideal **C**.

Complex **2d** did not give an isolatable protonation product. The final products—the hydrogenation product **1d** of the starting material **2d** and free 1,1-diphenylethane—may be explained by a partial decomposition of **2d** immediately after the addition of the acid, to give free 1,1-diphenylethene and some cobalt-containing species. The latter could be oxidized by the acid, thereby generating hydrogen radicals, which in turn hydrogenate the unsaturated side chain of diphenylethene both in the complex and in the free state. However, when less than the stoichiometric amount of acid was used for protonation, some of the starting material **2d** apparently did not become protonated nor hydrogenated during the course of the reaction. This could be a clue to that the reduction of the ligand actually proceeds via an unstable protonated species, which is more easily hydrogenated than **2d**. In addition, the organometallic decomposition products of **4a** were found to be the deprotonation and hydrogenation products **2a** and **1a**, which is in line with the above arguments.

(C) Cations $[(CpCo)_3(\mu_3$-α-methylstyrene)$]^+$ 2a$^+$. The ^{1}H NMR spectra of the crystalline material, which was obtained by protonation of **2a** with CF_3COOH and subsequent reaction with $NaBPh_4$, are typical of a paramagnetic complex. Therefore it can be ruled out that this product is **4a**$[BPh_4]^-$. Field desorption mass spectra only gave a parent ion at *m*/*z* 490, which is the mass of **2a**, whereas parent ions with *m*/*z* 491 were observed from freshly prepared salts of **4a**.

The crystal structure analysis does not immediately identify the bridging arene ligand. In particular, the nature of the side chain is not immediately obvious. However, the observed geometry can be rationalized by the assumption of a propen-2-yl side chain, which is disordered in two positions related by a 180° rotation around C(1)−C(7). The observed distances C(7)−C(8/9) [1.403(8) and 1.413(8) Å] compare well with the average length of the double and single carbon carbon bonds in the side chains of related μ_3-alkenylbenzene complexes (1.415(6) Å, side chain = propen-1-yl, complex **2b**,[7a,b] 1.405(9) Å, side chain = propen-2-yl, $[(CpCo)_3\{\mu_3$-(4-F)C_6H_4(C(Me)=CH_2)$\}]$ (**2e**)[8]). The distance C(1)−C(7) is with 1.475(6) Å close to the corresponding values

(17) (a) Seyferth, D. *Adv. Organomet. Chem.* **1976**, *14*, 97. (b) Seyferth, D.; Williams, G. H.; Nivert, C. L. *Inorg. Chem.* **1977**, *16*, 758. (c) Schilling, B. E. R.; Hoffmann, R. *J. Am. Chem. Soc.* **1978**, *100*, 6274; **1979**, *101*, 3456. (d) Edidin, R. T.; Norton, J. R.; Mislow, K. *Organometallics* **1982**, *1*, 561.

(18) McGlinchey, M. J.; Girard, L.; Ruffolo, R. *Coord. Chem. Rev.* **1995**, *143*, 331.

(19) Acampora, M.; Ceccon, A.; Dal Farra, M.; Giacometti, G.; Rigatti, G. *J. Chem. Soc., Perkin Trans. 2* **1977**, 483.

(20) Olah, G. A.; Yu, S. H. *J. Org. Chem.* **1976**, *41*, 1694.

in **2b** [1.461(5) Å] and **2e** [1.481(8) Å]. The angle between the planes of the μ_3-C_6 ring and the propen-2-yl side chain is also similar in **2a**$^+$ and in **2e** (24 vs 35°). We can therefore conclude that the crystals are the tetraphenylborate of **2a**$^+$, the one-electron oxidation product of **2a**.

As in **2e** and **3d**, the distortions from an ideal μ_3-η^2:η^2:η^2 coordination of the arene to the metal cluster can be related to repulsion of the sterically demanding side chain with the adjacent CpCo group.

(D) Molecular Orbital Calculations. Structure of 4a−c. Extended Hückel molecular orbital calculations were performed in order to understand and rationalize a few questions related to the experiments previously described. The different sites of protonation for **1** and **2** can be explained by our extended Hückel MO study. The HOMO of $[(CpCo)_3\{\mu_3\text{-}C_6H_5(C(H)=CH_2)\}]$ (**2′**) has a large LCAO amplitude on the β carbon atom of the vinyl substituent. This carbon also carries a substantial negative charge (Figure 3). Although these numbers must be taken carefully, owing to the qualitative nature of the method used, the trend is clear. Both charge and overlap control favor attack by the electrophile on the cobalt atoms for **1** and on the β carbon for **2**.

A search for the preferrred geometry of the protonated cations **4** and its comparison to the paramagnetic cation **2a**$^+$ was another principal aspect of our study.

The bonding of the benzene ligand to a trinuclear metal cluster has been studied in some detail. Some of us have previously investigated the interaction of benzene with the $(CpCo)_3$ cluster, using the approximate Fenske−Hall SCF method.[21] Our results have later been confirmed by several extended Hückel, Fenske−Hall, and *ab initio* studies on the valence isoelectronic derivatives $[\{(CO)_3M\}_3(\mu_3\text{-}C_6H_6)]$ (M = Ru, Os).[22] There is an electronic preference for a staggered conformation of the benzene relative to the metal triangle and for an alternation of stronger (shorter) and weaker (longer) bonds in the ring, the shorter bonds eclipsing the metal atoms. On the basis of crystal structure analyses of a considerable number of derivatives of both **1** and **2**, the experimental difference between mean values for the two types of endocyclic carbon carbon bonds is indeed about 0.03 Å.[11,12] The activation barrier for rotation of the ring relative to the triangular face of the cluster is fairly small.

Having these results in mind, we conclude that the structural preferences of the paramagnetic cations $[(CpCo)_3\{\mu_3\text{-}C_6H_5(C(R)=CH_2)\}]^+$ are of steric nature. This is evident from the comparison of the results for R = H and R = Me, the latter complex preferring a much larger deviation (30°) from the staggered geometry than the former (12°). As extended Hückel calculations tend to overestimate repulsions, it is more likely that the real angle is closer to 12°, in as good as possible agreement with the X-ray determined structure of **2a**$^+$.

The reasons favoring the bending away of the hydrogen atoms or other substituents on benzene ligands coordinated to triangular faces of clusters have been discussed before.[21,22] Indeed, the calculated total energy

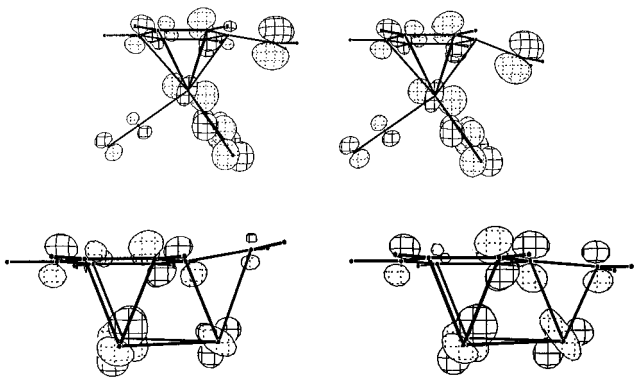

Figure 8. A molecular orbital relevant in the process of bending the $C_6H_5CH_2^+$ side chain: $[Cr(CO)_3(C_6H_5CH_2)]^+$ (top), 170 and 158°; $[(CpCo)_3(\mu_3\text{-}C_6H_5CH_2)]^+$ (bottom), 190 and 175°.

of the cations drops when the side chains are bent away from the metal cluster. Taken together, our calculations reproduce quite well the geometry of the paramagnetic cation **2a**$^+$ and therefore confirm its adequate assignment. Similar results are obtained for the neutral $[(CpCo)_3\{\mu_3\text{-}C_6H_5(C(H)=CH_2)\}]$ model, as might be expected.

Having ascertained that a paramagnetic cation such as **2**$^+$ fits the results of the structure obtained by X-ray methods, it remains to determine what the structure of the protonated derivatives **4** would be.

Our minimum energy structures, obtained with the extended Hückel and DFT methods, contrast that of the mononuclear benzyl cation complex $[Cr(CO)_3(C_6H_5\text{-}CH_2)]^+$.[19,23] For this compound, which we recalculated with the extended Hückel method as a calibration, the favored calculated slipping of the arene is only 0.14 Å, while the side chain prefers to bend *toward* the metal atom by 26°. The small differences relative to older calculations[23] reflect geometrical details and eventual parameter differences but confirm the analysis. Indeed, for a mononuclear complex, better overlap is achieved with this distortion which allows the seven carbon atoms of the arene to bind.

One of the orbitals responsible for this trend is shown in Figure 8, top. On the other hand, for the larger triangular cobalt cluster, a larger slip is favored and we can trace the tendency of the side chain to bend away from the metal in the orbital shown in Figure 8, bottom (the energy becomes 0.3 eV lower). It closely resembles the one for the Cr complex. The difference is that in some π orbitals the side chain carbon has not the same phase as the adjacent carbons and, therefore, the resulting bonding molecular orbital becomes Co−C antibonding when the arene slips. These repulsive interactions are relieved by the bending of the side chain away from the metal triangle. This overcomes some loss of bonding character in a few other cluster orbitals.

With a planar C_6 ring, the relatively large slip of the benzyl ligand would place the ring carbon *para* to the side chain at a large distance from the metal cluster. In our calculated structure, reasonable cobalt−carbon bond lengths involving this carbon atom and two cobalts are obtained by a folding of the benzyl ring (Figure 7). The μ_3-α,1-η^2:2−4-η^3:4−6-η^3-benzyl coordination so ob-

(21) Wadepohl, H.; Zhu, L. *J. Organomet. Chem.* **1989**, *376*, 115.
(22) (a) Gallop, M. A.; Gomez-Sal, M. P.; Housecroft, C. E.; Johnson, B. F. G.; Lewis, J.; Owen, S. M.; Raithby, P. R.; Wright, A. H. *J. Am. Chem. Soc.* **1992**, *114*, 2502. (b) Riehl, J.-F.; Koga, N.; Morokuma, K. *Organometallics* **1993**, *12*, 4788.

(23) Downton, P. A.; Sayer, B. G.; McGlinchey, M. J. *Organometallics* **1992**, *11*, 3281.

tained has much in common with that of the nonplanar μ_3-cycloheptatrienyl ligand in the cluster complex $[Co_4(CO)_6(\eta^5\text{-}C_7H_9)(\mu_3\text{-}1,2\text{-}\eta^2\text{:}3\text{-}5\text{-}\eta^3\text{:}5\text{-}7\text{-}\eta^3\text{-}C_7H_7)]$.[24] In both ligands, two η^3-enyl systems sharing a common carbon atom are coordinated to two cobalt atoms of the cluster, whereas the remaining two carbons (exocyclic in the former, endocyclic in the latter system) bind to the third metal.

A nonplanar η^7-coordinated benzyl ligand has also been found in the mononuclear complex $[Cp^*Zr(CH_2\text{-}Ph)_2]^+$.[25] In this complex, a boat-type conformation of the benzyl is attained. Bridging (μ-η^7) benzyl species have previously been detected on certain metal surfaces as the dehydrogenation products of toluene.[26] On the Pt(111) surface, a $\pi + \sigma$ bonded 1−6-η^6:α-η^1-coordination, where the aromatic sextet is retained, was suggested, on the basis of vibrational spectroscopy data.[26c] Such a species, where the methylene group is σ-bonded to the surface independently from the phenyl ring, would be quite different from the benzyl ligand in **4**.

Concluding Remarks

In the past we have elaborated on synthetic, structural, and dynamic aspects of the cluster complexes $[(CpCo)_3(\mu_3\text{-arene})]$ in some detail.[3,7,11,13] During the synthesis, the unsaturated side chain on the arene plays a crucial role in the assemblage of the tricobalt cluster on site of the arene.[27] However, it is not required for the stability of the complexes (once they have been formed), has a negligible influence on the interaction of the arene with the metal cluster, and is only a spectator as far as dynamic stereochemistry is concerned.[28]

In the present work we were able to show that the type of side chain (unsaturated enylic or saturated at C-α) does indeed determine the course of reaction with protonic acids. A rational for this behavior is given by the results of our MO studies. It must be kept in mind, however, that in the absence of serious attempts to determine the kinetic site of attack of the cluster by the electrophile, the above discussion is restricted to the thermodynamic products.

Experimental Section

General Procedures. All operations were carried out under an atmosphere of purified nitrogen or argon (BASF R3−11 catalyst) using Schlenk techniques. Solvents were dried by conventional methods. Petroleum ether refers to the fraction with bp 40−60 °C. The compounds $[(CpCo)_3(\mu_3\text{-}$isopropylbenzene$)]$ (**1a**), $[(CpCo)_3(\mu_3\text{-}p\text{-}$diethylbenzene$)]$ (**1b**), $[(CpCo)_3(\mu_3\text{-}$1,2-diphenylethane$)]$ (**1c**), and $[(CpCo)_3(\mu_3\text{-}$1,1-diphenylethane$)]$ (**1d**) were obtained as described previously by catalytic hydrogenation of the corresponding cluster complexes with μ_3-alkenylbenzene ligands.[3,11,29] The complexes $[(CpCo)_3(\mu_3\text{-}$α-methylstyrene$)]$ (**2a**), $[(CpCo)_3(\mu_3\text{-}\beta\text{-}$methylstyrene$)]$ (**2b**), $[(CpCo)_3(\mu_3\text{-}p\text{-}$methoxystyrene$)]$ (**2c**), and $[(CpCo)_3(\mu_3\text{-}$1,1-diphenylethylene$)]$ (**2d**) were prepared by published procedures.[7] Trifluoroacetic acid was destilled under vacuum prior to use.

NMR spectra were obtained with Bruker AC-200 (200.1 MHz for ^{1}H, 50.3 MHz for ^{13}C), Bruker AC-300 (300.1 MHz for ^{1}H, 75.46 MHz for ^{13}C), and Jeol FX-90Q (28.7 MHz for ^{11}B) instruments. ^{1}H and ^{13}C chemical shifts are reported vs $SiMe_4$ and were determined by reference to internal $SiMe_4$ or residual solvent peaks. The multiplicities of the ^{13}C resonances were determined using the DEPT or the *J*-modulated spin echo (JMOD) techniques. ^{11}B chemical shifts are referenced to external $BF_3\cdot OEt_2$. Mass spectra (positive ions) were measured in the electron impact ionization mode (EI) at 70 eV or using field desorption (FD) or chemical ionization (CI) with isobutane on Finnegan MAT 8230 and 4600 spectrometers.

In Situ Protonations. General Procedure. Solutions of ca. 20 mg (ca. 0.05 mmol) of $[(CpCo)_3(\mu_3\text{-arene})]$ in 0.4 mL of CD_2Cl_2 were made up in NMR tubes which were then sealed with septum stoppers. A 10−15 μL (0.1−0.2 mmol) amount of CF_3COOH was added to the solution in several portions through the septum stopper. Between additions of acid, the mixture was agitated and ^{1}H NMR spectra were taken. When complete protonation was observed, all volatiles were removed from the samples under reduced pressure and the residues redissolved in CD_2Cl_2. Apart from the absence of the resonance due to free CF_3COOH, the ^{1}H spectra so obtained did not differ significantly from those measured in the presence of excess acid.

Preparative-Scale Protonations. General Procedure for Reactions with Trifluoroacetic Acid. The acid was added dropwise to a stirred solution of the cluster complex in 50−80 mL of CH_2Cl_2. All volatiles were then removed under reduced pressure. The oily residues were generally spectroscopically pure products. Attempted recrystallization from CH_2Cl_2 usually led to the separation of the product as a brown oil.

Preparation of $[H(CpCo)_3(\mu_3\text{-}$1,2-diphenylethane$)]^+$ (3c). (A) Trifluoroacetate Salt. A 970 mg amount of a brown oil (1.45 mmol, 98% based on **3c**$[CF_3COO]^-$) was obtained from 820 mg (1.48 mmol) of **1c** and 170 mg (1.49 mmol, 115 μL) of CF_3COOH. MS (FD): *m*/*z* (rel intensity) 555 (M^+, 100). MS (CI): *m*/*z* (rel intensity) 555 (M^+, 5), 314 (9), 190 (12), 189 (100, $[Cp_2Co]^+$), 182 (78), 124 (14, $[CpCo]^+$).

(B) Hexafluorophosphate Salt. A mixture of 400 mg (0.72 mmol) of **1c** and 0.2 mL of HPF_6 solution (75% in water) in 50 mL of toluene was stirred at room temperature. After 24 h the brown precipitate was filtered off and washed with toluene. Yield: 360 mg (71%) of spectroscopically pure **3c**$[PF_6]^-$; the pale brown powder liquifies within a few minutes to give a brown oil. ^{1}H NMR (300 MHz, in $CDCl_3$, ambient temp): $\delta = -14.71$ (s, 1H, Co_3H), 2.36 ("t", 2H, CH_2), 2.76 ("t", 2H, CH_2) 4.3−4.4 (m, 5H, μ-arene-H), 5.28 (s, 15H, 3Cp), 7.0−7.3 (m, Ph).

(C) Tetraphenylborate Salt. A 120 mg (0.17 mmol) amount of **3c**$[PF_6]$ was stirred with 60 mg (0.17 mmol) of $NaBPh_4$ in 10 mL of CH_2Cl_2 for 4 h. A colorless precipitate was filtered off, and the filtrate was crystallized at −20 °C. Yield: 60 mg of black microcrystalline **3c**$[BPh_4]$ (41%). ^{1}H NMR (300 MHz, in $CDCl_3$, ambient temp): $\delta = -14.85$ (s, 1H, Co_3H), 2.23 ("t", 2H, CH_2), 2.71 ("t", 2H, CH_2) 4.0−4.1 (m, 5H, μ-arene-H), 4.96 (s, 15H, 3Cp), 6.9−7.5 (m, Ph). ^{13}C NMR (75.5 MHz, in $CDCl_3$, ambient temp): $\delta = 39.4$ (CH_2), 42.7 (μ-arene-CH), 43.4 (μ-arene-CH), 43.9 (CH_2), 46.9 (μ-arene-CH), 68.6 (μ-arene C-*ipso*), 83.1 (Cp), 121.9 (BPh_4 CH), 125.6 (BPh_4 CH), 126.5 (Ph-CH), 128.54 (Ph-CH), 128.65 (Ph-CH), 136.4 (BPh_4 CH), 140.4 (Ph C-*ipso*), 164.4 ($J_{BC} = 49$ Hz, BPh_4 C-*ipso*). ^{11}B NMR (in $CDCl_3$): $\delta = -5.77$.

Preparation of $[H(CpCo)_3(\mu_3\text{-}$1,1-diphenylethane$)]^+$ Trifluoroacetate Salt (3d$[CF_3COO]^-$). Following the general

(24) Wadepohl, H.; Gebert, S.; Pritzkow, H.; Braga, D. *Chem. Eur. J.*, submitted for publication.
(25) Pellecchia, C.; Immirzi, A.; Pappalardo, D.; Peluso, A. *Organometallics* **1994**, *13*, 3773.
(26) (a) Friend, C. M.; Muetterties, E. L. *J. Am. Chem. Soc.* **1981**, *103*, 773. (b) Tsai, Min-Chi; Muetterties, E. L. *J. Phys. Chem.* **1982**, *86*, 5067. (c) Avery, N. R. *J. Chem. Soc., Chem. Commun.* **1988**, 153.
(27) Wadepohl, H.; Büchner, K.; Pritzkow, H. *Organometallics* **1989**, *8*, 2745.
(28) It has to be noted, however, that the activation barrier for arene rotation depends on the steric bulk of the side chain(s). In some cases, the seemingly paradox situation arises that derivatives with more bulky substituents have lower barriers.[13]
(29) Herrmann, M. Dissertation, Heidelberg, 1991.

procedure (*vide supra*), 120 mg of a brown oil (1.45 mmol, 100% based on **3d**[$CF_3COO]^-$) was obtained from 100 mg (0.18 mmol) of **1d** and 1.48 g (13.0 mmol, 1 mL) of CF_3COOH. ^1H NMR (300 MHz, in $CDCl_3$, ambient temp): $\delta = -14.2$ (s, 1H, Co_3H), 1.36 (d, $J_{HH} = 7.2$ Hz, 3H, CH_3), 3.54 (q, $J_{HH} = 7.2$ Hz, 1H, $CHCH_3$), 4.3−4.4 (m, 2H, μ-arene-H), 4.62 (t, $J_{HH} = 5.9$ Hz, 1H, μ-arene-H), 4.70 (d, $J_{HH} = 6.2$ Hz, 1H, μ-arene-H), 4.81 (d, $J_{HH} = 6.5$ Hz, 1H, μ-arene-H), 5.42 (s, 15H, 3Cp), 7.2 (m,[a] Ph). ^1H NMR (200 MHz, in $CDCl_3$, 230 K): $\delta = -14.1$ (s, 1H, Co_3H), 1.34 (d, $J_{HH} = 7.2$ Hz, 3H, CH_3), 3.50 (q, $J_{HH} = 7.2$ Hz, 1H, $CHCH_3$), 4.26−4.36 (2t, 2H, μ-arene-H), 4.57 (t, $J_{HH} = 5.9$ Hz, 1H, μ-arene-H), 4.65 (d, $J_{HH} = 6.2$ Hz, 1H, μ-arene-H), 4.79 (d, $J_{HH} = 6.5$ Hz, 1H, μ-arene-H), 5.38 (s, 5H, Cp), 5.40 (s, 5H, Cp), 5.46 (s, 5H, Cp), 7.1−7.3 (m,[a] Ph) (a: overlap with solvent resonance). MS (FD): *m/z* (rel intensity) 555 (M^+, 100). MS (CI): *m/z* (rel intensity) 555 (M^+, 0.1), 258 (3), 190 (16), 189 (100, $[Cp_2Co]^+$), 182 (9), 168 (16), 134 (15), 124 (22, $[CpCo]^+$), 115 (19), 114 (20).

Preparation of [(CpCo)$_3${μ_3-$C_6H_5C(CH_3)_2$}]$^+$ Trifluoroacetate Salt (4a[$CF_3COO]^-$). Following the general procedure (*vide supra*), 700 mg of a brown oil (1.16 mmol, 98% based on **4a**[$CF_3COO]^-$) was obtained from 580 mg (1.18 mmol) of **2a** and 135 mg (1.18 mmol, 91 μL) of CF_3COOH. MS (FD): *m/z* (rel intensity) 491 (M^+, 100).

Preparation of [(CpCo)$_3${μ_3-$C_6H_5C(H)(C_2H_5)$}]$^+$ Tetraphenylborate Salt (4b[$BPh_4]^-$). A 148 mg (1.30 mmol, 100 mL) amount of CF_3COOH was added dropwise to a stirred solution of **2b** (520 mg, 1.06 mmol) in 50 mL of CH_2Cl_2 at −50 °C. The solution was slowly warmed to room temperature (ca. 1 h). $NaBPh_4$ (380 mg, 1.11 mmol) was then added. A colorless precipitate was filtered off after 1 h. The filtrate was layered with petroleum ether. On cooling to −20 °C **4b**[$BPh_4]^-$ separated as black microcrystals (370 mg, 43%). ^1H NMR (200 MHz, in CD_2Cl_2): $\delta = 0.9$ (m, 1H, CH_2), 1.24 (dd, $J_{HH} = 7.2$ Hz, 6.0 Hz, 3H, CH_3), 1.3 (m, CH_2), 1.93 (dt, $J_{HH} = 6.0$, 1.7 Hz, 1H, μ-arene-H), 4.67 (dt, $J_{HH} = 6.2$ Hz, 1.2 Hz, 1H, μ-arene-H), 4.85 ("s", Cp, C-αH), 4.98 (s, Cp), 5.2 (m, 2H, μ-arene-H), 5.29 (s, 5H, Cp), 5.85 (td, $J_{HH} = 5.8$ Hz, 1.4 Hz, 1H, μ-arene-H), 6.91 (t, $J_{HH} = 7.0$ Hz, 4H, Ph), 7.05 (t, $J_{HH} = 7.2$ Hz, 8H, Ph), 7.2−7.4 (m, 8H, Ph). ^{13}C NMR (75.5 MHz, in CD_2Cl_2): $\delta = 15.3$ (CH_3), 25.7 (CH_2), 37.3 (CH), 41.5 (CH), 50.2 (CH), 51.0 (CH), 51.3 (CH), 80.0 (C-α), 83.4 (Cp), 84.6 (Cp), 86.1 (Cp), 122.2 (BPh_4 CH), 126.0 (BPh_4 CH), 129.2 (μ-arene C-*ipso*), 136.4 (BPh_4 CH), 164.4 (q, $J_{BC} = 49$ Hz, BPh_4 C-*ipso*). ^{11}B NMR (in $CDCl_3$): $\delta = -2.5$. MS (FD): *m/z* (rel intensity) 491 (M^+, 100).

Attempted Preparation of [(CpCo)$_3${μ_3-$C_6H_5C(CH_3)_2$}]$^+$ Tetraphenylborate Salt. A 240 mg (2.11 mmol, 160 mL) amount of CF_3COOH was added dropwise to a stirred solution of 1.0 g (2.04 mmol) of **2a** in 50 mL of CH_2Cl_2 at −50 °C. The solution was slowly warmed to room temperature (ca. 1 h). $NaBPh_4$ (700 mg, 2.04 mmol) was then added. A brown precipitate formed which redissolved after a few minutes. A colorless precipitate was filtered off after 1 h. The filtrate was layered with petroleum ether and stored at −20 °C. After 4 d a small amount of black crystals and some amorphous precipitate was removed by filtration. The crystals were used for X-ray structure determination. A total of 320 mg of **2a**$^+$[$BPh_4]^-$ was subsequently obtained by repeated layering of the mother liquor with petroleum ether and storage at −20 °C.

Crystal Structure Determination of [H(CpCo)$_3$(μ_3-η^2:η^2:η^2-1,1-diphenylethane)]$^+$[$CF_3COO]^-$·H_2O (3d[$CF_3COO]^-$·H_2O) and [(CpCo)$_3$(μ_3-η^2:η^2:η^2-α-methylstyrene)]$^+$[$BPh_4]^-$·CH_2Cl_2 (2a$^+$[$BPh_4]^-$·CH_2Cl_2). Single crystals of **3d**[$CF_3COO]^-$·H_2O were grown from an aqueous solution by slow evaporation of solvent under nitrogen at room temperature. Small single crystals of **2a**$^+$[$BPh_4]^-$·CH_2Cl_2 precipitated at −20 °C from a solution in dichloromethane which was layered with petroleum ether, as described above. The crystals were mounted in Lindemann capillary tubes. Intensity data were collected on a Siemens STOE four-circle diffractometer at ambient temperature and corrected for Lorentz, polarization, and absorption effects (Table 7). The structures were solved by direct methods and refined by full-matrix least squares based on F^2 using all measured unique reflections. All non-hydrogen atoms were given anisotropic displacement parameters.

Table 7. Details of the Crystal Structure Determinations of [H(CpCo)$_3$(μ_3-η^2:η^2:η^2-1,1-diphenylethane)]$^+$[$CF_3COO]^-$·H_2O (3d[$CF_3COO]^-$·H_2O) and [(CpCo)$_3$(μ_3-η^2:η^2:η^2-α-methylstyrene)]$^+$[$BPh_4]^-$·CH_2Cl_2 (2a$^+$[$BPh_4]^-$·CH_2Cl_2)

	3d[$CF_3COO]^-$·H_2O	**2a**$^+$[$BPh_4]^-$·$0.5CH_2Cl_2$
formula	$C_{31}H_{32}Co_3F_3O_3$	$C_{48}H_{46}BCo_3$·$0.5CH_2Cl_2$
cryst habit, color	box, black	box, black
cryst size (mm)	0.17 × 0.28 × 0.34	0.35 × 0.42 × 0.75
cryst system	monoclinic	monoclinic
space group	$P2_1/n$	$C2/c$
a (Å)	8.996(6)	18.942(9)
b (Å)	23.659(15)	17.686(9)
c (Å)	12.756(8)	24.178(12)
β (deg)	98.67(5)	105.36(3)
V (Å^3)	2684(3)	7811(7)
Z	4	8
M_r	686.36	852.91
d_c (g·cm^{-3})	1.699	1.451
F_{000}	1400	3528
μ(Mo Kα) (mm^{-1})	1.887	1.362
X-radiation, λ (Å)	Mo Kα, graphite monochromated, 0.710 69	
data collect temp	ambient	
2θ range (deg)	3-50	3-50
hkl range	−10/10, 0/28, 0/15	−22/21, 0/21, 0/28
reflcns measd		
total	4975	7128
unique	4753	6884
obsd [$I \geq 2\sigma(I)$]	2990	3615
abs corr	empirical	empirical
T_{min}, T_{max}	0.82, 1.00	0.565, 0.662
params refined	413	531
R-values	0.060	0.045
R (obsd reflecns only)		
w*R*2 (all reflecns) ($w = 1/[\sigma^2(F) + (AP)^2 + BP]$	0.174	0.110
A, *B*	0.0952, 0	0.0348, 9.59
P	$[\max(F_o^2,0) + 2F_c^2]/3$	
GooF	1.093	1.003

Three independent sets of intensity data were collected from three different crystals of **2a**$^+$[$BPh_4]^-$·$0.5\ CH_2Cl_2$. The structure was solved with all three data sets. Only the data set which had the largest number of observed reflections was used for refinement.

Some of the hydrogen atoms (those on the μ_3-arene rings, the hydride H1, and the methyne hydrogen on C7 in **3d**) were located from difference Fourier maps and refined with isotropic atomic displacement parameters. All other hydrogen atoms were input in calculated positions. Methyl groups were treated as rigid groups. In **2a**$^+$, the termini of the side chain were treated as rigid methyl groups with site occupation factors 5/6 for all six hydrogen atoms. The rotational orientation of the methyl groups was taken from partial Fourier syntheses. Due to severe rotational disorder, the C−F and F···F distances of the CF_3 group were restrained to 1.32(3) and 2.17(5) Å, respectively, during refinement.

The calculations were performed using the programs SHELXS-86 and SHELXL-93.[30] Graphical representations were drawn with the ORTEP-II program.[31]

Molecular Orbital Calculations. (a) Semiempirical Calculations. All calculations were done using the extended Hückel method[32] and modified H_{ij}'s[33] with the CACAO pro-

(30) (a) SHELXS-86, Sheldrick, G. M. *Acta Crystallogr.* **1990**, *A46*, 467. SHELXL-93: Sheldrick, G. M. Universität Göttingen, 1993.
(31) Johnson, C. K. *ORTEP-II*; Report ORNL-5138; Oak Ridge National Laboratory: Oak Ridge, TN.
(32) (a) Hoffmann, R. *J. Chem. Phys.* **1963**, *39*, 1397. (b) Hoffmann, R.; Lipscomb, W. N. *J. Chem. Phys.* **1962**, *36*, 2179, 3489.

gram.[34] The basis set for the metal atoms consisted of *n*s, *n*p, and (*n* − *1*)d orbitals. The s and p orbitals were described by single Slater-type wave functions, and the d orbitals were taken as contracted linear combinations of two Slater-type wave functions. Standard parameters were used for H, C, and O, and the following for Co (H_{ii}/eV, ζ): 4s, −9.54, 2.000; 4p, −4.51, 2.000; 3d, −12.48, 5.55 (ζ_1), 2.10 (ζ_2), 0.5679 (C_1), 0.6059 (C_2). The following were used for Cr (H_{ii}/eV, ζ): 4s, −8.66, 1.700; 4p, −5.24, 1.70; 3d, −11.22, 4.950 (ζ_2), 1.80 (ζ_2), 0.5058 (C_1), 0.6747 (C_2).

Idealized models were used for the clusters studied. The metallic fragment $(CpCo)_3$ and the arene ligands were based on the geometries described in this work for **3d** and **2a**$^+$. The following distances (Å) were used: Co−Co 2.45, Co−C_{Cp} 2.12, Co−arene(normal) 1.75, C−C 1.40, C−H 1.08. The orientation of the Cp rings relative to the Co_3 plane was optimized.

(b) DFT Calculations. The DFT calculations reported in this work are based on the ADF package (Amsterdam density functional).[35] The program is characterized by the use of a density fitting procedure to obtain accurate Coulomb and exchange potentials, by an accurate and efficient numerical integration of the effective one-electron Hamiltonian matrix elements and by the use of frozen core orbitals. The molecular orbitals were expanded in an uncontracted triple-ζ STO basis set for all elements. Polarization functions were added. For geometry optimizations a local spin density aproximation (LSDA) together with the Vosko−Wilk−Nusair parametrization[36] for correlation was used. A nonlocal gradient correction was introduced after the SCF cycles to compute a posteriori a correction to the energy. All energy calculations were performed with the nonlocal PW91[37] corrections.

Acknowledgment. This work was supported by the Deutsche Forschungsgemeinschaft (DFG) and the Fonds der Chemischen Industrie (FCI). We thank the DFG for the award of a Heisenberg Fellowship (to H.W.) and the FCI for a studentship (to C.J.). P.M.E.L. thanks JNICT for financial support. Support for P.M.E.L. and M.J.C. by the European Union (Human Capital and Mobility scheme) is gratefully acknowledged.

Supporting Information Available: Tables of X-ray parameters, positional and thermal parameters, and bond distances and angles (23 pages). Ordering information is given on any current masthead page.

OM9605692

(33) Ammeter, J. H.; Bürgi, H.-B.; Thibeault, J. C.; Hoffmann, R. *J. Am. Chem. Soc.* **1978**, *100*, 3686.
(34) Mealli, C.; Proserpio, D. M. *J. Chem. Educ.* **1990**, *67*, 39.
(35) (a) Baerends, E. J.; Ellis, D. E.; Ros, P. *Chem. Phys.* **1973**, *2*, 42. (b) Baerends, E. J.; Ros, P. *Int. J. Quantum Chem.* **1978**, *S12*, 169.
(36) Vosko, S. H.; Wilk, L.; Nusair, M. *Can. J. Phys.* **1980**, *58*, 1200.
(37) Perdew, J. P.; Wang, Y. *Phys. Rev. B* **1986**, *33*, 8800.